

High-level natural radionuclides from the Mandena deposit, South Madagascar

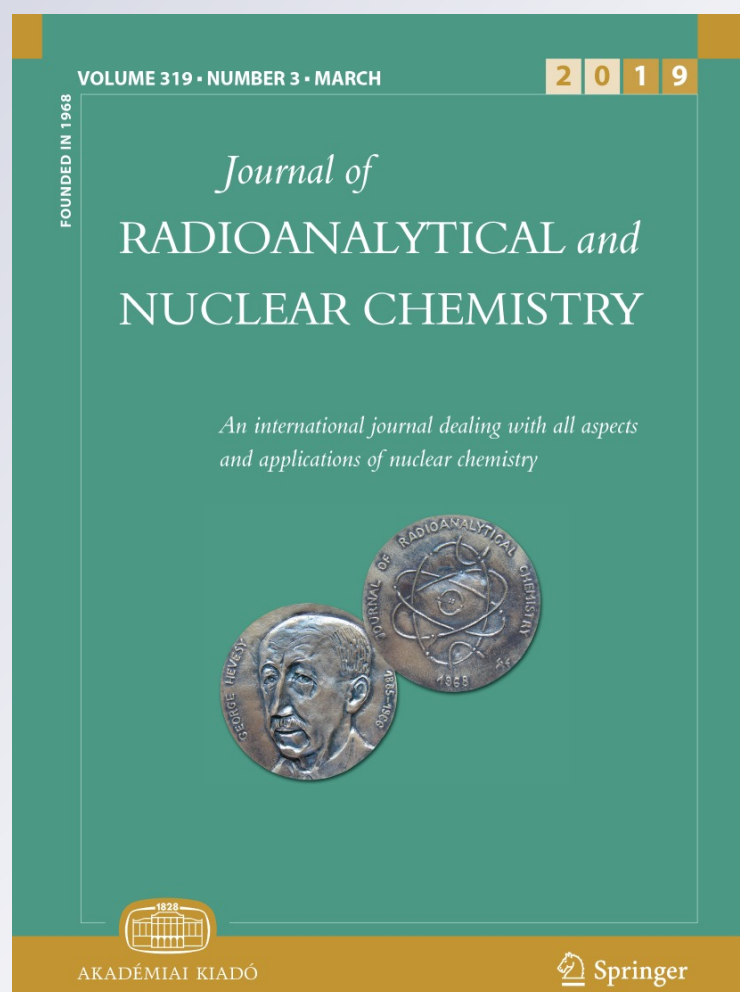
**Duong Van Hao, Chau Nguyen Dinh,
Paweł Jodłowski & Tibor Kovacs**

Journal of Radioanalytical and Nuclear Chemistry

An International Journal Dealing with All Aspects and Applications of Nuclear Chemistry

ISSN 0236-5731
Volume 319
Number 3

J Radioanal Nucl Chem (2019)
319:1331-1338
DOI 10.1007/s10967-018-6378-z



Your article is protected by copyright and all rights are held exclusively by Akadémiai Kiadó, Budapest, Hungary. This e-offprint is for personal use only and shall not be self-archived in electronic repositories. If you wish to self-archive your article, please use the accepted manuscript version for posting on your own website. You may further deposit the accepted manuscript version in any repository, provided it is only made publicly available 12 months after official publication or later and provided acknowledgement is given to the original source of publication and a link is inserted to the published article on Springer's website. The link must be accompanied by the following text: "The final publication is available at link.springer.com".



High-level natural radionuclides from the Mandena deposit, South Madagascar

Duong Van Hao¹ · Chau Nguyen Dinh² · Paweł Jodłowski³ · Tibor Kovacs⁴

Received: 8 August 2018 / Published online: 12 December 2018
© Akadémiai Kiadó, Budapest, Hungary 2018

Abstract

The ²³⁸U, ²²⁶Ra and ²³²Th contents of six samples from the Mandena black sand placer deposit were determined by gamma-ray spectrometry and varied from 2280 to 4600 Bq/kg, 1530 to 2900 Bq/kg and 11,600 to 25,400 Bq/kg, respectively. The activity concentration of ²³²Th is significantly higher than ²³⁸U and there is no equilibrium between ²³⁸U and ²²⁶Ra. Due to the gamma interferences at the line 1461 keV and very high ²²⁸Ac activity, the ⁴⁰K was calculated through potassium analyzed using ICP-AES and varied from 1 to 19 Bq/kg. The calculated gamma absorbed dose rate ranged from 7700 to 16,700 nGy/h.

Keywords Gamma-ray spectrometry · Beach black sand · High content of thorium and uranium · Disequilibrium · Interfering peaks · ICP-AES

Introduction

In many regions in the world, there are regions with elevated natural radioactivity. Among these regions there are black beach sand placers which often are rich in heavy minerals. They were formed by long-time weathering and erosion of different rock types, transported and deposited along beaches. There are many studies concerning beach sand placers especially respecting: Chhatrapur and Erasama of Orissa in India, Rosetta in Egypt, placer in South–East Bangladesh, Ilha Grande of Brazilian southeastern, Kavala, Sithonia Chalkidiki, Maronia, Samothraki and Mykonos of Greece [1–13]. All the mentioned publications reported very high gamma terrestrial and inhalation dose rate ranged from a few 100–1000 nGy/h and near 1–10 mSv/y, respectively. Sand beach placer is often composed of monazite, ilmenite, zircon, rutile, garnet and so on. They contain high

amounts of thorium and uranium. The study of the radioactive elements concentration in beach sand placer enables to calculate the gamma absorbed dose rate, which principally is related to the concentration of radionuclides of uranium, thorium series and potassium ⁴⁰K. The gamma absorbed dose rate at 1 m above ground is often estimated using the formulae [14]:

$$D(\text{nGy/h}) = 0.0417 \cdot K + 0.462 \cdot Ra + 0.604 \cdot Th \quad (1)$$

where K, Ra and Th are activity concentration of ⁴⁰K, ²²⁶Ra and ²³²Th of the sample expressed in (Bq/kg).

The Mandena black sand placer in East–South Madagascar is the typical deposit rich in heavy metals. The ilmenite mining has been provided by the Rio Tinto Corporation at the mentioned deposit since 2008, the annual exploited yield of ilmenite ore varies from 750,000 to 1,000,000 tons [15]. The mining and processing the titanium and rare earth elements can cause a big hazard on environment [15]. The hazard is not only in destroy of living natural resources, but also in agricultures. According with the Kill and Franchi report [16] the neighboring Fort Dauphin ilmenite deposits are located under the littoral forest with 42 plants and at least 14 invertebrate species nowhere found in the World. Therefore many international organizations such as Non-Governmental Organization (NGO), Business and Biodiversity Offset Programmer (BBOP), International Finance Corporation and others are willing and ready to rescue the

✉ Duong Van Hao
haodnth@gmail.com

¹ University of Mining and Geology (UMG), Hanoi, Vietnam

² Faculty of Geology and Geophysics and Environmental Protection, AGH University of Science and Technology, Kraków, Poland

³ Faculty of Physics and Applied Computer Science, AGH University of Science and Technology, Krakow, Poland

⁴ Institute of Radiochemistry and Radioecology, University of Pannonia, Veszprem, Hungary

destroyed forests and natural living resource together with social enlargement for inhabitants [16].

The authors of the study determined the concentration of ^{40}K , ^{238}U , ^{226}Ra and ^{232}Th in several samples collected from Mandena black sand placer in East–South Madagascar, and attempted to calculate the gamma absorbed dose rate for inhabitants and to explain some specific phenomena observed in the studied materials.

Materials and methods

Studied area

The Mandena black sand placer is located in the East–South Madagascar (Fig. 1). The area of this deposit is near 9 square km and its estimated resource amounts to about 20 million tons of ilmenite, rutile and zircon minerals in total. The average concentration of the ilmenite, monazite, zircon and other matrix minerals is 66.7%, 2.3%, 2.8% and 28.3%, respectively [17]. There is a very high content of both thorium and uranium in the placer materials but very low potassium content. The six samples, each was approximately 600 g, were collected from the east boundary to the centre of Mandena deposit. The samples were marked from S1 to S6 and the distance between two neighboring samples amounts to near 500 m [17]. Then the collected samples were analyzed

at AGH University of Science and Technology, Krakow, Poland.

Gamma-ray spectrometry analysis

The sample was milled until the grains became less than 2 mm, then it was dried in an oven at 120 °C for 24 h to ensure that moisture was completely removed, then weighed and packed in an aluminum cylindrical beaker and sealed to prevent the escape of radon. The weighed and tightly sealed samples were left for at least 21 days to reach secular equilibrium between ^{226}Ra and ^{222}Rn as well as its daughters (mostly ^{214}Bi and ^{214}Pb).

The activity concentration was determined using a semiconductor HPGe detector (Canberra GX4020) with 42% relative efficiency. The energy resolution of the spectrometer at the line 1333 keV (^{60}Co) is near 2 keV. As standard samples, reference materials RG produced by the International Atomic Energy Agency (IAEA) were used.

Samples were measured in cylindrical geometry 48 cm³ (sample diameter 70 mm, height 12.5 mm), directly on the detector. The measurement time of samples amounted near 50 h. A detail description of the methodology is presented in [19].

^{40}K was quantified using its 1461 keV emission, ^{238}U via its daughter $^{234\text{m}}\text{Pa}$ 1001 keV emission line. ^{226}Ra was determined via its daughter ^{214}Bi (609 keV, 1120 keV and

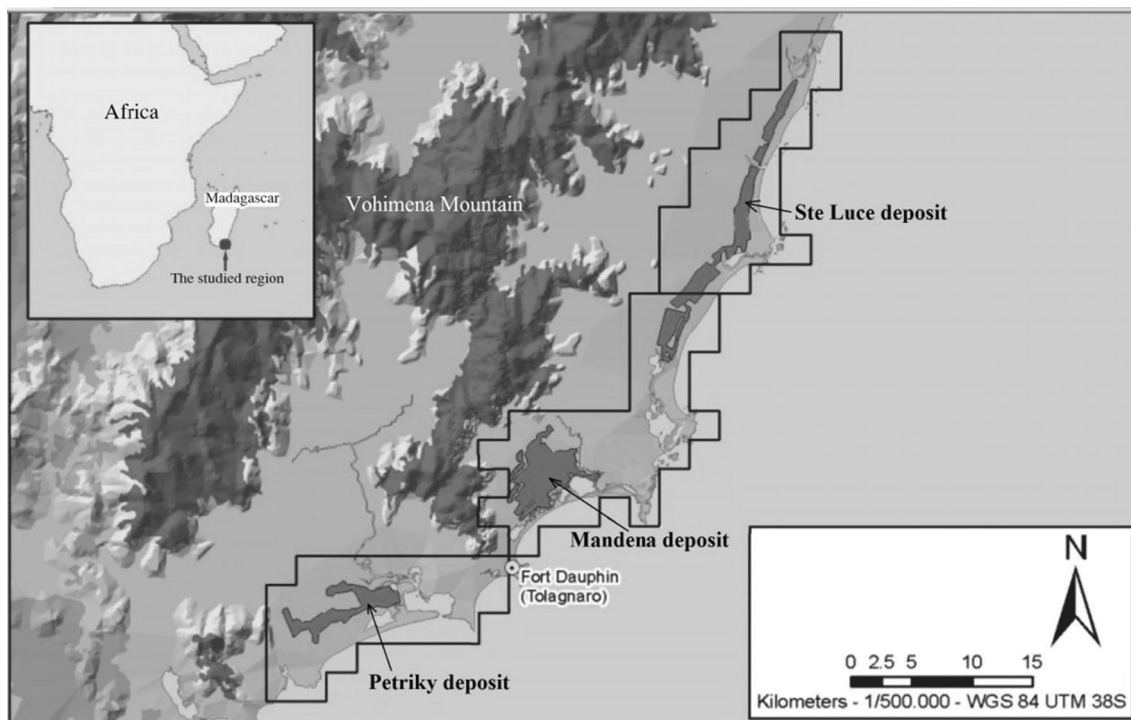


Fig. 1 Sketch of the black sand deposits in East–South Madagascar [18]

1764 keV) emissions. ^{232}Th was assayed via the emissions of its daughters ^{228}Ac (911 keV, 967 keV) and ^{208}Tl (583 keV, 2614 keV), with which it may be assumed to be in secular equilibrium (Table 1). The self-attenuation correction accounting the difference of density of the samples

and standard ones was introduced follow method proposed by Debertin [20, 21].

Due to the very high ^{232}Th , high ^{238}U concentration and very low ^{40}K concentration in the studied samples, it is necessary to consider the interferences for several lines used in the calculation (Table 1, Fig. 2).

Table 1 The principal gamma ray energies, used for determination of natural radionuclides by gamma spectrometry

Nuclide measured	Nuclide emitting	Gamma energy (keV)	Emission probability of the photon I_γ (%) [22]	Gamma detection efficiency ϵ^a [19]	Interfering lines ^b [22]: energy (keV) – nuclide – I_γ (%) – contribution in the peak ^c [%]
^{40}K	^{40}K	1460.8 ^d	10.55	0.01702	1459.1 ^d – ^{228}Ac – 0.87; 98 1458.5 – $^{234\text{m}}\text{Pa}$ – 0.0019 – 0.04
^{232}Th	^{228}Ac	911.2	26.2	0.02510	
		968.9	15.9	0.02382	
	^{208}Tl	583.2	30.6	0.03607	
		2614.4	35.9	0.01055	
^{238}U	$^{234\text{m}}\text{Pa}$	1001.0 ^e	0.847	0.02314	1000.7 ^e ^{228}Ac – 0.0054 – 3
^{226}Ra	^{214}Bi	609.3	45.5	0.03480	610.6 – ^{228}Ac – 0.024 – 0.3
		1120.3	15.0	0.02109	
		1764.5	15.9	0.01452	

^aThe spectrometer efficiency for the cylindrical measurement geometry 48 cm³ and for sand matrix (density 1.389 g/cm³)

^bInterfering peaks from other series were taken into account only

^cContribution in the peak was calculated for the following concentrations: ^{40}K —20 Bq/kg, ^{238}U —2000 Bq/kg, ^{226}Ra —2000 Bq/kg, ^{232}Th —10,000 Bq/kg

^dCoincidence-summing correction 1.00 and 1.06 respectively

^eCoincidence-summing correction 1.00 and 1.22 respectively

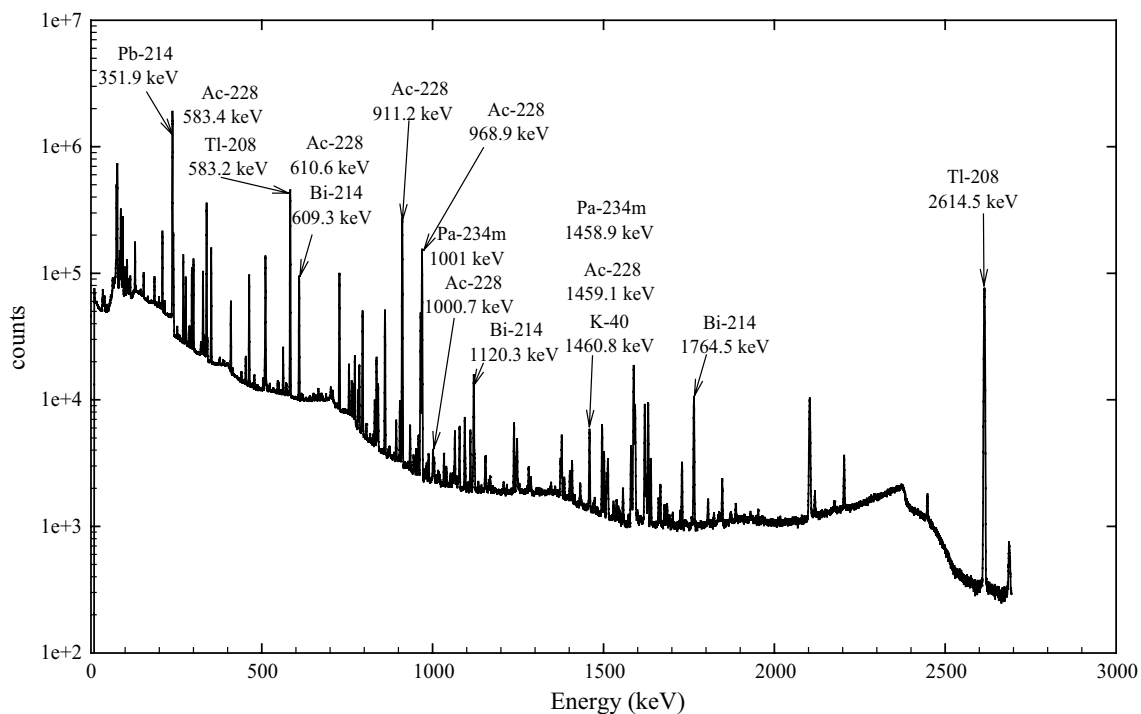


Fig. 2 The gamma spectrum of S5 sample measured through 35 h

Significant interference occurs for the following lines:

For the 1001.0 keV ^{234m}Pa line (I_γ 0.847%), used for determination of ^{238}U , interfering line 1000.7 keV from ^{228}Ac (I_γ 0.0054%) is present in the spectrum.

For the 1460.8 keV line, used for determination of ^{40}K (I_γ 10.55%), interfering line 1459.1 keV from ^{228}Ac (I_γ 0.87%) is present in the spectrum; contribution of ^{234m}Pa 1458.5 keV interfering line (I_γ 0.0019%) is negligible.

Corrections to interfering lines (on the example of ^{40}K) were introduced as follows. Count rate originating from the ^{40}K can be calculated from the formula:

$$N_{\text{K40}}^{1460} = N_{\text{total}}^{1460} - N_{\text{Ac228}}^{1460} = N_{\text{total}}^{1460} - A_{\text{Ac228}} \cdot I_{\gamma, \text{Ac228}, 1459.1} \cdot \epsilon_{1460} \cdot (1/C_{\text{c}, \text{Ac228}, 1459.1}) \quad (2)$$

where N_{K40}^{1460} —the count number originating from ^{40}K , N_{total}^{1460} —the count number in the peak 1460 keV of both from ^{40}K and ^{228}Ac , N_{Ac228}^{1460} —calculated count number originating from ^{228}Ac , A_{Ac228} — ^{228}Ac activity, $I_{\gamma, \text{Ac228}, 1459.1}$ —the emission probability of the photon of energy 1459.1 keV by ^{228}Ac , ϵ_{1460} —the spectrometer efficiency for 1460 keV, $C_{\text{c}, \text{Ac228}, 1459.1}$ —coincidence-summing correction for 1459.1 keV line of ^{228}Ac .

ICP-AES method

The sample was digested with mixture of chloric, nitric and hydrofluoric acids. The chemical composition of samples was analyzed using an ICP-AES PerkinElmer Optima 7300 DV spectrometer at the AGH UST. The ICP-AES calibrated with a multi-element standard solution of the Merck® Company. The induced couple plasma instrument worked with a cooling argon flow of 14 L/min, a reflected RF power of 1350 W, both auxiliary gas and nebulizer flow rates of 1.0 L/min, a sample intake of 0.8 mL/min. The detection limit depends on the individual element and ranged from a few to tens ppb with 3% of uncertainty. K element concentration was recalculated to ^{40}K activity concentration (cf. Table 2).

Results and discussion

Due to the very high ^{232}Th and very low ^{40}K concentration in analyzed material, the contribution of 1459.1 keV ^{228}Ac line in (1460.8 keV + 1459.1 keV) peak is close to 100%. As a result, after subtraction of the ^{228}Ac contribution, the ^{40}K concentration is determined with very high uncertainty, larger than the measured value. For example, the ^{40}K activity for S1 sample determined by this method equals to -52 ± 70 Bq/kg. This means that with such a large disparity between the ^{232}Th and ^{40}K concentration ($^{232}\text{Th} \gg ^{40}\text{K}$), determination of ^{40}K is not possible using gamma-ray spectrometry. Therefore ^{40}K concentration was determined through K element using the ICP-AES method.

The authors attempted to assess detection limit for ^{40}K concentration for analyzed black sands using gamma spectrometry. In the assessment a simplified formula was used for the low limit of detection proposed by Currie [23].

$$L_D = 4.26 \cdot \sqrt{N_{\text{bckg}}} \quad (3)$$

where N_{bckg} is the count number of background.

For ^{40}K concentration equal to detection limit

$$N_{\text{K40}}^{1460} = 4.26 \cdot \sqrt{N_{\text{bckg}}} = 4.26 \cdot \sqrt{N_{\text{Ac}, 1459.1} + N_{\text{bckg}, 1460}} \quad (4)$$

$$a_{\text{K40}} \cdot m \cdot I_{\gamma, \text{K40}, 1460.8} \cdot \epsilon_{1460} \cdot (1/C_{\text{c}, \text{K40}, 1460.8}) \cdot t = 4.26 \cdot \sqrt{a_{\text{Ac228}} \cdot m \cdot I_{\gamma, \text{Ac}, 1459.1} \cdot \epsilon_{1460} \cdot (1/C_{\text{c}, \text{Ac228}, 1459.1}) \cdot t + N_{\text{bckg}, 1460}} \quad (5)$$

where $N_{\text{Ac}, 1459.1}$ —calculated count number in the peak 1460 keV originating from ^{228}Ac (line 1459.1 keV), $N_{\text{bckg}, 1460}$ —spectrometer background in the peak 1460 keV, a_{K40} , a_{Ac228} —activity concentration of ^{40}K and ^{228}Ac , respectively (Bq/kg), m —sample mass, t —measurement time.

For spectrometer used (cf. data in Table 2), sample mass about 0.130 kg and measurement time 50 h:

$$a_{\text{K40}} \geq 0.18 \cdot \sqrt{a_{\text{Ac228}}} = 0.18 \cdot \sqrt{a_{\text{Th232}}} \quad (6)$$

Table 2 ^{226}Ra , ^{238}U , ^{232}Th and ^{40}K activity concentration of the black sand samples measured by gamma-ray spectrometry and ICP-AES and calculated gamma absorbed dose rates 1 m over the black sand layer

Sample	^{40}K (Bq/kg)	^{238}U (Bq/kg)	^{226}Ra (Bq/kg)	$^{238}\text{U}/^{226}\text{Ra}$	^{232}Th (Bq/kg)	$^{232}\text{Th}/^{238}\text{U}$	Dose rate (nGy/h)
S 1	13.9 ± 0.4	2280 ± 110	1530 ± 46	1.49 ± 0.09	$11,600 \pm 350$	5.08 ± 0.29	7700 ± 210
S 2	8.6 ± 0.3	2580 ± 130	1630 ± 49	1.58 ± 0.09	$12,700 \pm 380$	4.91 ± 0.28	8400 ± 230
S 3	19.0 ± 0.6	2800 ± 140	1700 ± 51	1.65 ± 0.10	$13,300 \pm 400$	4.74 ± 0.27	8790 ± 240
S 4	8.5 ± 0.3	2640 ± 130	1670 ± 50	1.58 ± 0.09	$12,900 \pm 390$	4.89 ± 0.28	8560 ± 240
S 5	5.3 ± 0.2	3550 ± 180	2060 ± 62	1.72 ± 0.10	$16,300 \pm 490$	4.59 ± 0.27	$10,800 \pm 300$
S 6	0.89 ± 0.3	4600 ± 230	2900 ± 87	1.59 ± 0.09	$25,400 \pm 760$	5.51 ± 0.32	$16,700 \pm 460$

where a_{Th232} is activity concentration of ^{232}Th ; in calculation secular equilibrium in thorium series was assumed and spectrometer background was considered to be negligible.

It means that rough low limit of detection for ^{40}K , for analyzed black sands equals about 20 Bq/kg.

The ^{40}K activity concentration in analyzed black sands is lower than 19 Bq/kg, the ^{238}U concentration ranges from 2280 to 4600 Bq/kg (180–370 ppm), the ^{226}Ra from 1530 to 2900 Bq/kg and ^{232}Th from 11,600 to 25,400 Bq/kg (2800–6200 ppm) (Table 2).

The concentration of ^{238}U and ^{232}Th in the samples are several tens to several hundred times higher than the average concentrations of the mentioned isotopes in the Earth crust (~40 Bq/kg—[14]). Such high concentrations of the uranium and thorium are also observed in beach sand deposits in Brasilia and India and other regions in the World [1, 13].

The activity concentration of ^{232}Th is higher than ^{238}U by five times, equivalent to fifteen times in mass (Table 2). The phenomena is the common for the beach sand deposits [1–13]. In the beach sand the zircon, garnet, spinel, sillimanite, monazite, anatase, rutile, titanite, leucoxene are major minerals, which often bear thorium element. Thorium in these minerals is very resistant against the weathering conditions. On the other hand uranium present in these minerals easily transfers from the compound of U^{4+} to that of U^{6+} and became very easily to be dissolved in water and transported to the other places [24].

The equilibrium starting from the ^{228}Ra was found in thorium series based on ^{228}Ac and ^{208}Tl measurements (cf. paragraph Gamma-ray spectroscopy analysis).

The disequilibrium between ^{238}U and ^{226}Ra was found. $^{238}U/^{226}Ra$ activity ratio equals to about 1.6. Though ^{238}U and ^{226}Ra belong to the uranium series, in general for the

Table 3 Concentrations of the elements in the samples S1, S5 and S6 analyzed by ACME laboratory (ICP-ES/MS)

Element	Unit	S1	S5	S6	Element	Unit	S1	S5	S6
Si	wt%	6.93	na	na	Pr	ppm	790	993	1600
Al	wt%	0.980	0.380	0.270	Nd	ppm	2830	>2000	>2000
Fe	wt%	20.6	18.2	18.5	Sm	ppm	384	499	782
Mg	wt%	0.540	0.280	0.250	Eu	ppm	1.85	2.30	3.70
Ca	wt%	0.530	0.170	0.140	Gd	ppm	203	211	326
Na	wt%	0.089	0.119	0.065	Tb	ppm	14.6	20.1	33.4
K	wt%	0.041	0.020	0.010	Dy	ppm	44.0	57.6	93.4
Ti	wt%	25.5	8.50	8.45	Ho	ppm	3.77	3.30	4.80
P	wt%	0.367	0.272	0.400	Pr	ppm	790	993	1600
Mn	ppm	2320	2550	2540	Er	ppm	9.00	9.20	15.1
Cr	ppm	280	207	206	Tm	ppm	1.53	0.800	1.10
Ba	ppm	840	960	990	Yb	ppm	11.8	5.90	8.70
Sc	ppm	52.0	36.1	34.7	Lu	ppm	1.98	0.300	0.300
Be	ppm	3	<1	<1	Mo	ppm	0.40	10.4	10.2
Co	ppm	41.9	43.1	42.9	Cu	ppm	5.70	35.2	36.6
Cs	ppm	<0.1	<0.1	<0.1	Pb	ppm	61.0	237	287
Ga	ppm	16.9	29.3	35.5	Zn	ppm	14.0	262	296
Hf	ppm	745	13.9	13.4	Ni	ppm	1.40	15.5	14.6
Nb	ppm	>1000	762	744	As	ppm	0.700	13.0	10.3
Rb	ppm	1.500	0.900	0.500	Cd	ppm	<0.1	<0.1	<0.1
Sn	ppm	13.0	8.80	9.00	Sb	ppm	0.600	0.700	0.660
Sr	ppm	95.0	80.0	73.0	Bi	ppm	<0.1	0.460	0.420
Ta	ppm	62.7	24.2	22.9	Ag	ppm	<0.1	na	na
Th	ppm	2820	1350	1130	Au	ppm	0.700	na	na
U	ppm	124	125	188	Hg	ppm	0.020	na	na
V	ppm	680	398	424	Tl	ppm	<0.1	<0.1	<0.1
W	ppm	11.0	9.70	8.50	Se	ppm	<0.5	1.10	2.80
Zr	ppm	31,000	453	459	Te	ppm	na	<0.05	<0.05
Y	ppm	140	123	183	In	ppm	na	0.880	0.850
La	ppm	3140	>2000	>2000	Re	ppm	na	<0.002	<0.002
Ce	ppm	6900	>2000	>2000	Li	ppm	na	6.30	7.70

na not analyzed

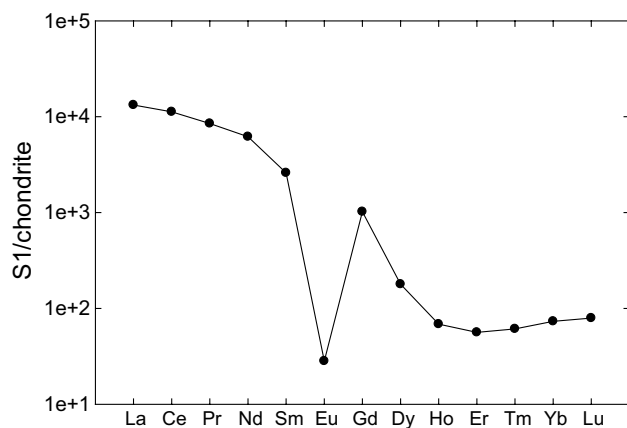


Fig. 3 The pattern of REE in S1 sample

weathered rocks and for the soil there is disequilibrium between them. This fact can be related with: (1) difference in geochemical properties of the elements. Radium always occurs in state of 2+, this element can be leached by water through various weathering processes; on the other hand, uranium can occur in 4+, 5+ and 6+ depending on the redox condition; (2) in the uranium series ^{226}Ra is formed after three alpha decays, so according to the nuclear recoil, ^{226}Ra can be removed from the rock e.g. to the water.

In order to geochemically characterize, the samples S1, S5 and S6 were analyzed at the certificated ACME laboratory in Canada, the obtained results are summarized in Table 3. Due to the similar concentration of ^{238}U , ^{226}Ra and ^{232}Th sample S1 has been found to be representative of the group of samples S1 ÷ S4.

Taking into account that in 1 mg of K there is 0.0304 Bq of ^{40}K , the concentrations of potassium obtained by ACME are comparable with that analyzed by ICP-AES carried out by the AGH-UST laboratory. Generally the ore deposit is very rich in titanium (from 8.5 to 25.5 wt%) and in Σ REE (15,000 ppm) especially LREE. Figure 3 is showing the ratios of rare elements in sample S1 to the concentrations of these elements in chondrite. For samples S5 and S6 REE pattern is similar.

There is Eu negative anomaly and deposit material is very rich in Σ REE (1.4 wt%) with very high Σ LREE/ Σ HREE ratio (near 51), suggesting origin from the weathering processes on the igneous magmatic formations [25, 26], but the guess should be checked by isotopes' analyze on the deposit minerals. The main trace elements are Pb, Cr, As, Zn, Cd, Cu, and Hg. Among the mentioned elements only Cr and Cu (Table 3) in the analyzed samples exceeded the regulatory limits for these metals in uncontaminated soil equal to 100 and 10 ppm, respectively [27].

Table 4 Statistic values of ^{40}K , ^{238}U , ^{232}Th concentration and gamma absorbed dose rate D for some high background radiation areas

Element	Parameter	Bihac, Bosnia and Herzegovina ^a [28]	Tamilnadu, India ^b [29]	Guangdong, China ^c [30]	Mandena black sand placer ^a
^{238}U (Bq/kg)	Min	43	bl ^d	284	2280
	Max	651,500	172	721	4600
	Average	54	8.3	524	3070
	Std.	5.2	2.8	180	780
^{232}Th (Bq/kg)	Min	22	bl ^d	176	11,600
	Max	53	1397	396	25,400
	Average	41	54	291	15,300
	Std.	6.5	3.3	86	4700
^{40}K (Bq/kg)	Min	193	bl ^d	1606	0.89
	Max	424	532	2803	19
	Average	367	192	2239	9.4
	Std.	77	18	450	5.8
D (nGy/h)	Min	49	nd ^e	304	7700
	Max	73	128	689	16,700
	Average	64	57	511	10,200
	Std.	6.2	4.0	154	3060

^aData were directly taken from the paper [28] and from this work

^bThe data for a given parameter were calculated as an algebraic average of the values of the this parameter for analyzed layers, e.g. $\text{min} = \Sigma \text{min}_i / n$, where i —layer index, n —number of the layers

^cThe data for a given parameter were calculated as a weighted average of the values of this parameter; the length of the measured profile was taken as a weight, e.g. $\text{min} = \Sigma(\text{length}_i * \text{min}_i) / \Sigma \text{length}_i$; where i —profile index

^dbl below the limit of detection

^end not determined

Using the formulae (1) and the results obtained by ICP-AES and gamma spectrometry for ^{40}K , ^{226}Ra and ^{232}Th the gamma absorbed dose rates 1 m over the black sand layer were calculated and summarized on Table 2. The gamma absorbed dose rates are very high and varied from 7700 nGy/h to above 16,000 nGy/h ($7 \div 16 \mu\text{Gy/h}$) with 10,200 nGy/h of average. This value is six and eight fold higher than that on Chhatrapur beach placer of Orissa India (1625 nGy/h) and East Rosetta beach sand in Egypt (1200 nGy/h), respectively [3, 13]. Using the data of the study deposit and data published in the papers [28–30], the statistic values of ^{238}U , ^{232}Th , ^{40}K and gamma absorbed dose rates for the areas of high background radiation—such as Bihac city in Bosnia and Herzegovina [28], Tamilnadu coast India [29], and granitic uranium deposit in Guangdong China [30]—were estimated and summarized in Table 4.

The data in Table 4 show that in the Mandena deposit the average uranium and thorium concentrations are extremely high and near 50, 350, 6 (for uranium) and 400, 300, 50 (for thorium) times higher than in the Bihac, Tamilnadu and Guangdong areas respectively. In consequence of such as high concentrations of Th and U, the gamma absorbed dose rates in the Mandena deposit is very high. Thorium and uranium series contribution in the absorbed dose rate in Mandena deposit is about 90% and 10%, respectively; ^{40}K contribution is negligible.

The calculated average gamma absorbed dose rate in this deposit is near 200 times higher than the worldwide average natural dose rate (59 nGy/h) [14].

Conclusions

The Mandena black sand placer deposit in Madagascar is very rich in titanium and rare earth elements. The deposit materials are probably formed by the weathering processes on the intrusive magmatic rocks. The activity concentrations of ^{232}Th , ^{238}U as well as ^{226}Ra in the deposit are very high and range from several thousand to few ten thousand Bq/kg. The thorium-bearing minerals are very resistant against the weathering processes, in consequence thorium activity is the highest. Due to characteristics of the beach sand deposit and geochemical properties of uranium and radium elements, there is disequilibrium between ^{238}U and ^{226}Ra . The activity concentration of ^{40}K is very low in comparison with ^{232}Th and ^{238}U . Due to interference effect of the gamma radiation emitted from the ^{228}Ac (^{232}Th series), determination of ^{40}K is practically not possible using gamma-ray spectrometry; at such high thorium and uranium concentration the low detection limit of ^{40}K for spectrometer used is about 20 Bq/kg. The gamma absorbed dose rate 1 m over analyzed black sand layer is very high and mostly contributed from the thorium series.

Acknowledgements The work was partly supported by the Ministry of Science and Higher Education (Grant Nos. 11.11.140.645 and 11.11.220.01). The authors would like to express their thankfulness to Drs Beata Ostachowicz and Jakub Nowak for their useful discussions. Many thanks to the colleague from Madagascar, Ms. Lantoarindriaka for providing samples.

References

- Alencar AS, Freitas AC (2005) Reference levels of natural radioactivity for the beach sands in a Brazilian southeastern coastal region. *J Radiat Meas* 40:76–83
- Freitas AC, Alencar AS (2004) Gamma dose rates and distribution of natural radionuclides in sand beaches, Ilha Grande Southeastern Brazil. *J Environ Radioact* 75:211–223
- Mohanty AK, Sengupta D, Das SK, Saha SK, Van KV (2004) Natural radioactivity and radiation exposure in the high background area at Chhatrapur beach placer deposit of Orissa, India. *J Environ Radioact* 75:15–33
- Nada A, Abd EM, Abu ZH, El-Asy IE, Mostafa SMI, Abd EA (2012) Correlation between radionuclides associated with zircon and monazite in beach sand of Rosetta, Egypt. *J Radioanal Nucl Chem* 291:601–610
- Papadopoulos A, Christofides G, Koroneos A, Stoulos S (2014) Natural radioactivity distribution and gamma radiation exposure of beach sands from Sithonia Peninsula. *Central Eur J Geosci* 6:229–242
- Papadopoulos A, Koroneos A, Christofides G, Papadopoulos L, Tzifas I, Stoulos S (2016) Assessment of gamma radiation exposure of beach sands in highly touristic areas associated with plutonic rocks of the Atticocycladic zone (Greece). *J Environ Radioact* 162:235–243
- Papadopoulos A, Koroneos A, Christofides G, Stoulos S (2014) Natural radioactivity distribution and gamma radiation exposure of beach sands close the granitoids of NE Chalkidiki, Greece. In: Proceedings of the 10th international congress of the heli-geographical society, pp 805–814
- Papadopoulos A, Koroneos A, Christofides G, Stoulos S (2015) Natural radioactivity distribution and gamma radiation exposure at beach sands close to Kavala pluton, Greece. *Open J Geosci* 1:407–422
- Papadopoulos A, Koroneos A, Christofides G, Stoulos S (2015) Natural radioactivity distribution and gamma radiation exposure of beach sands close to Maronia and Samothraki plutons, NE Greece. *Geol Balc* 43:99–107
- Primal P, Narayana Y (2014) Studies on the seasonal variation and vertical profiles of natural radionuclides in high background radiation areas of Kerala on the south west coast of India. *J Radioanal Nucl Chem* 302:813–817
- Sulekha R, Sengupta D, Guin R, Saha SK (2009) Natural radioactivity measurements in beach sand along southern coast of Orissa, eastern India. *Environ Earth Sci* 59:593–601
- Kumar R, Mahur AK, Rao NS, Sengupta D, Prasad R (2008) Radon exhalation rate from sand samples from the newly discovered high background radiation area at Erasama beach placer deposit of Orissa, India. *J Radiat Meas* 43:15–33
- Abb El Wahab M, El Nahas HA (2013) Radionuclides measurements and mineralogical studies on beach sands, East Rosetta Estuary, Egypt. *Chin J Geochem* 32:146–156
- United Nations Scientific Committee on the Effects of Atomic Radiation (UNSCEAR) (2000) Report to the general assembly,

- with scientific annexes (UNCEAR 2000), vol 1. Annex B - exposures from natural radiation sources, pp 84–141
15. A report by Harbinson R, Head of Environment at Panos London (2007). https://friendsoftheearth.uk/sites/default/files/downloads/development_recast.pdf. Accessed 28 June 2018
 16. Kill J, Franchi G (2016) Rio Tinto in Madagascar: a mine destroying the unique biodiversity of the littoral zone of Fort Dauphin. WRM and Re: Common, pp 1–32
 17. Lantoarindriaka A (2016) Master thesis: “Mineral composition of heavy fraction from beach sand and technological sand process, Fort-Dauphin, Madagascar”. In: AGH UST, Krakow, Poland
 18. Gaylord L (2016) Rio Tinto QIT Madagascar minerals report
 19. Jodłowski P, Kalita SJ (2010) Gamma-ray spectrometry laboratory for high-precision measurements of radionuclide concentrations in environmental samples. *Nukleonika* 55:143–148
 20. Jodłowski P (2006) Self-absorption correction in gamma-ray spectrometry of environmental samples—an overview of methods and correction values obtained for the selected geometries. *Nukleonika* 51:21–25
 21. Debertin K, Helmer RG (1988) Gamma- and X-ray spectrometry with semiconductor detectors. North-Holland Publications, Amsterdam
 22. DDEP, Decay Data Evaluation Project. http://www.nucleide.org/DDEP_WG/DDEPdata.htm. Accessed 20 Jan 2018
 23. Currie LA (1995) Nomenclature in evaluation of analytical methods including detection and quantification capabilities. *Pure Appl Chem* 67:1699–1723
 24. Drever J (1997) The geochemistry of natural waters. Prentice Hall, New Jersey
 25. Hoatson DM, Jaireth S, Mieziotis Y (2011) The major rare earth element deposits of Australia: geological setting, exploration, and resources. *Geosc Aust* 204:192
 26. Alexandre P, Kyser K, Layton-Matthews D, Yoy B (2015) Chemical composition of natural uraninite. *Can Mineral* 53:595–622
 27. Wuana RA, Okieimen FE (2011) Heavy metals in contaminated soils: a review of sources, chemistry, risks and best available strategies for remediation. *ISRN Ecol*. <https://doi.org/10.5402/2011/402647>
 28. Pehlivanovic B, Avdic S, Gazdic I, Osmanovic A (2016) Measurement of natural environmental radioactivity and estimation of population exposure in Bihac, Bosnia and Herzegovina. *J Radioanal Nucl Chem*. <https://doi.org/10.1007/s10967-016-5155-0>
 29. Punniyakotti J, Ponnusamy V (2017) Depth-wise distribution of ^{238}U , ^{232}Th and ^{40}K in sand samples of high background radiation areas (Tamilnadu coast), India. *J Radioanal Nucl Chem*. <https://doi.org/10.1007/s10967-017-5167-4>
 30. Wang J, Liu J, Chan Y, Song G, Chaen D, Xiao T, Wu S, Chen F, Yin M (2016) Technologically elevated natural radioactivity and assessment of dose to workers around a granitic uranium deposit area, China. *J Radioanal Nucl Chem* 1:1. <https://doi.org/10.1007/s10967-016-4809-2>